QF Modelling of Electro-Pulse-Therapy

Persson, Bertil R

Published in:
Acta Scientiarum Lundensia

2019

Document Version:
Publisher's PDF, also known as Version of record

Volume ASL 2019-001

Citation: (Acta Scientiarum Lundensia)

Persson, B. R. R., (2019). **QF Modelling of Electro-Pulse-Therapy**
Acta Scientiarum Lundensia, Vol. 2019-001, pp. 1-17, ISSN 1651-5013
(corrected version 2021-02-01)

Contact:
Bertil Persson PhD, MDhc, professor em
Mellanvångsvägen 7, 22355 Lund, Sweden
Mobil: +46720099122
Skype Namn: bertilrrpersson
bertil_r.persson@med.lu.se
bertilrrpersson@gmail.com
http://www2.msf.lu.se/b-persson/
http://orcid.org/0000-0002-5502-5972
https://www.youtube.com/watch?v=RzDesNluwnI&list=PL-jR3_adm3Ez0ZkH3LtaOS-orU6jfCB30&index=48&t=0s

QF MODELLING OF ELECTRO-PULSE-THERAPY

BERTIL RR PERSSON, prof.em.

Medical Radiation Physics
Lund University, 221 85 Lund, Sweden
e-mail: bertil_r.persson@med.lu.se

Abstract

In electro-pulse therapy treatment, only the cells exposed to a sufficiently strong electric field will respond immediately. The tumour cells that are permeabilized become much more accessible to hydrophilic molecules since these are normally rejected by the membrane barrier. The anticancer agent Bleomycin has proven to be the most potent drug in electro-pulse therapy and is the one often used in electro-pulse chemotherapy. However, cisplatin, another anticancer agent has also been found to be effective in electro-pulse chemotherapy.

Usually, needle electrodes are used for clinical treatment of tumours with Electro-pulse Chemotherapy. A short 100 microsecond pulse with a field-strength of about 1000 V/cm is applied between a pair of electrodes inserted in the tissue to be treated. After the initial pulse, the conductivity in the tissue close to the needle electrodes increase extensively.

The aim is to investigate this effect of the initial pulse on the distribution of potential, electric field, current density and absorbed power density of the following pulses. The present investigation has been possible to perform by using the evaluation grant of QuickField Professional program kindly submitted by the QuickField Support Team.

According to the result of the present QF simulation, the average pulse strength in the centre between the electrodes will increase above the recommended 1000 V/cm after the initial pulse, causing a high degree of non-reversible electroporation in the target volume by following pulses of the same amplitude.

Key Words:
electro-pulse therapy, tumour, permeabilization, membrane, Bleomycin, chemotherapy, Cisplatin, needle electrodes, electric field-strength,1000 V/cm, QuickField

1. Electro-pulse Chemo-Therapy (EpCT)

1.1 Historical development of Electro-pulse Chemo-Therapy (EpCT)

The possibility of using the electroporation effect for enhanced transport of anticancer drug across the cell membrane was first reported by Okino and Mohri 1987. They treated hepatocellular carcinoma (AH-109A) in Donryu rats by administration 5 mg Bleomycin intra-muscularly and exposed the tumours for an electric pulse with an amplitude of 5 kV/cm and 2 ms duration. At four days after the treatment, the tumour size had decreased significantly. While tumours treated only with electric impulse or Bleomycin showed no decreased in tumour growth. They suggested that electro-pulse chemo therapy should produce better results than chemotherapy alone (Okino and Mohri, 1987, Okino et al., 1992).

The first clinical trial with EECT was performed on head and neck tumours by Mir and colleagues in France, 1991 (Mir *et al*., 1991). Application of electric pulses *in vivo* used to augment the chemotherapeutic efficiency in cancer treatment has commonly been termed, ECT as an abbreviation for electro chemotherapy.
Nordenström 1998 developed electrochemical therapy (EChT) as a minimally invasive electrotherapeutic technique, using direct current for the treatment of cancer and haemangioma tumours. The acronym, ECT is also associated with *Electro Convulsive Therapy* used in psychiatry for treatment of depression.

In this presentation, EpCT is preferred as an abbreviation for *Electro-pulse Chemotherapy*. This novel mode of tumour treatment has been employed mostly for subcutaneous and cutaneous malignancies (Mir et al., 1998, Heller et al., 1998). However, the EpCT treatment of soft-tissue sarcomas (Hyacinthe et al., 1999), Glioma in the brain (Salford et al., 1993), liver tumours (Jaroszeski et al., 1997a, Jaroszeski et al., 1997b, Chazal et al., 1998, Ramirez et al., 1998) and the pancreas(Jaroszeski et al., 1999) has shown very promising results. Enhanced delivery of Bleomycin using electric fields for the effective treatment of skin malignancies has become synonymous to electro-pulse chemotherapy (Heller et al., 1997).

In electro-pulse chemotherapy treatment, only the cells exposed to a sufficiently strong electric field will respond immediately. The tumour cells that are permeabilized become much more accessible to hydrophilic molecules since these are normally rejected by the membrane barrier. Bleomycin, a very toxic anticancer agent, has proven to be the most potent drug in EpCT and is by far the one quite often used, but cisplatin, another anticancer agent has also been found to be effective.

Usually, needle electrodes are used in clinical treatment of tumours with Electro-pulse Chemotherapy by applying an electric pulse with a field-strength of about 1000 V/cm between a pair of electrodes inserted in the tissue to be treated. After the initial pulse has been applied, the conductivity distribution in the tissue close to the needle electrodes change extensively due to the inhomogeneous electric field distribution. The aim of this study is to model the effect of the increased conductivity close to the electrodes on the distribution of the electric-field between the electrodes.

The aim of the present work is to investigate the effect of the conductivity change after the initial pulse on the electric field distribution between the electrodes of the following pulse. This investigation has

been possible to perform by using the evaluation grant of QuickField Professional program kindly submitted by the QuickField Support Team.

2. OF-Modelling of field, current and power distribution in tissue

2.1 Modelling parameters

Modelling of field, current and power distribution in tissue is performed using QuickField, Finite-Element Analysis System, Version 6.3.2 (Tera Analysis Ltd. http://quickfield.com). QuickField is a program developed by Tera Analysis Ltd., Knasterhovvej 21, DK-5700 Svendborg, Denmark. In the program, the problems of current distribution are described by the Poisson's equation for scalar electric potential *U*.

With the problems of DC conduction, the field sources are external currents supplied to the boundary of a conductor. QuickField provides the possibility to specify external current density at the edges or at a specific vertex.

For problems of DC conduction, the QuickField postprocessor calculates the following set of local and integral physical quantities:

Components of the electric field vector **E**

The vector of electric field intensity E is defined as: $\bar{\boldsymbol{E}} = -\ \boldsymbol{grad}\ \mathrm{U}$

For planar 2D or 3D cases $E_x = -\frac{\partial U}{\partial x},\ E_x = -\frac{\partial U}{\partial y},\ E_z = -\frac{\partial U}{\partial z}$

For axisymmetric case $E_z = -\frac{\partial U}{\partial z},\ E_r = -\frac{\partial U}{\partial r}$

The DC electric current density **j** can be obtained from the equation. $\bar{\boldsymbol{j}} = \sigma \cdot \bar{\boldsymbol{E}} = -\sigma \cdot \boldsymbol{grad}\ \mathrm{U}$

where σ is the electric conductivity tensor

Absorbed power density (P_V, W.m^{-3}) in a volume V:

$$P_V = \oint_V (\boldsymbol{E^2} \cdot \boldsymbol{\sigma}) dV = \oint (\boldsymbol{E} \cdot \boldsymbol{j}) dV$$

Specific Absorbed Energy Rate (SAR, W.kg^{-1}; J.kg^{-1}.s^{-1}) in a volume V m^3 with the density ρ kg.m^{-3}:

$$SAR = \oint_V (\boldsymbol{E} \cdot \boldsymbol{j}) \cdot \rho^{-1} \cdot dV$$

Specific Absorbed Energy, i.e. Absorbed dose (SAE J.kg^{-1}) in a volume V with the density ρ kg.m^{-3} and exposure time t s.

$$SAE = \oint_V (\boldsymbol{E} \cdot \boldsymbol{j}) \cdot \rho^{-1} \cdot t \cdot dV$$

In a static system the temperature increases by Joule heating produced in a volume V is:

$$\Delta T = \text{SAE} / c_p$$

Where c_P is the specific heat capacities of the substance in the volume
Specific heat capacity of water (liquid): c_P = 4185.5 [J.kg^{-1}.°C^{-1}] (15 °C, 101.325 kPa)
Specific heat capacity of muscle issues is about 3421 ± 460 [J.kg^{-1}.°C^{-1}] {Hasgall, 2015 #5293

Temperature increase in living tissue depend strongly on the blood circulation which strives to maintain the temperature to 37°C. According to Pennes bioheat equation the temporal temperature change $\frac{\partial T}{\partial t}$ in arterial blood depends on the energy conductivity $\kappa\frac{d^2T}{dr^2}$ in the tissue, blood perfusion-rate v_b, metabolic rate MR, and the specific absorbed Power rate (SAR) dissipated by the electric pulses SAR (W.m^{-3}).

$$\rho \cdot c_b \cdot \frac{\partial T}{\partial t} = \kappa\frac{d^2T}{dx^2} + \kappa\frac{d^2T}{dy^2} + \kappa\frac{d^2T}{dz^2} + v_b \cdot c_b \cdot (37 - T) + MR + \text{SAR(x,y,z)}$$

Where

ρ	density ≈1060 kg.m^{-3}
c_b	specific heat capacity of blood ≈4000 J.kg^{-1}.°C^{-1}
κ	thermal conductivity ≈0.5 W.m^{-1}.°C^{-1}
v_b	blood perfusion rate ≈0.5 kg.m^{-3}.s^{-1}
MR	metabolic energy rate ≈33800 W.m^{-3}
SAR	specific absorbed Power rate W.m^{-3}

2.2 Dielectric properties of tissue

The Foundation for Research on Information Technologies in Society (ITIS) has an excellent database for the dielectric properties of various human tissues:
https://www.itis.ethz.ch/virtual-population/tissue-properties/database/dielectric-properties/

The figure 2-1 shows **relative permittivity** the frequency region 1 Hz – 1 GHz for muscle tissue derived from the ITIS database.

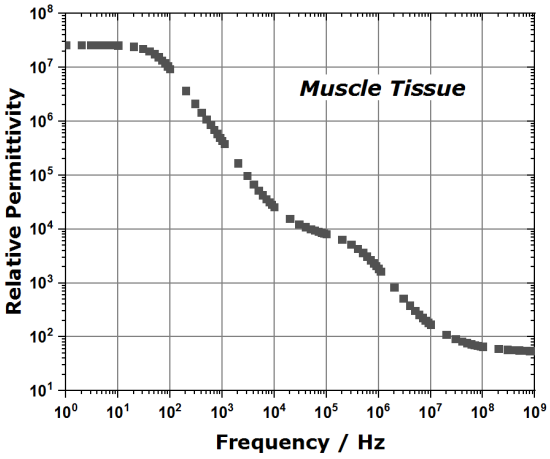

Figure 2-1
Relative permittivity of Muscle tissue in the frequency region of 1 Hz – 1 GHz
(Log_{10}/Log_{10} –scale)

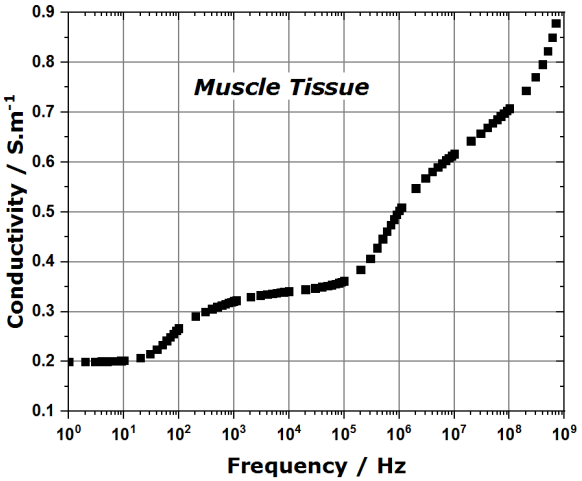

Figure 2-2
Conductivity of Muscle tissue in the frequency rage of 1 Hz – 1 GHz
(Log_{10} x/Lin y–scale)

The figures 2-2 shows the conductivity in Siemens per m ($S.m^{-1}$) in the frequency region 1 Hz – 1 GHz for muscle tissue derived from the ITIS database.

3. QF MODELLING RESULTS

3.1 Horizontal distribution of U, E, J and P_v at the initial pulse

3.1.1 Potential distribution U

Potential **U** profile between two needle electrodes with a diameter of 1mm inserted into muscle tissue with conductivity 0.20 S/m. The electrodes of steel with a conductivity of $6.2 \cdot 10^6$ S/m were separated 8 mm with an applied voltage of 1000 V at the left electrode and 0 V at the right.

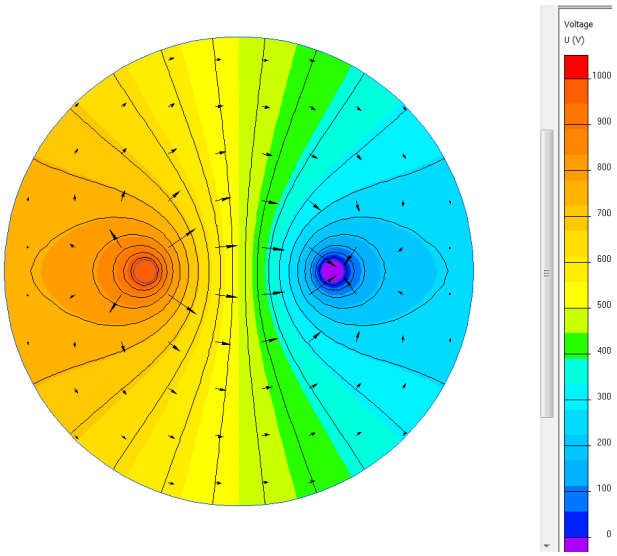

Figure 3-1
Distribution of potential U with an applied voltage of 1000 V over two electrodes of 1 mm diam. and 8 mm electrode spacing inserted in tissue with conductivity 0.2 S/m.

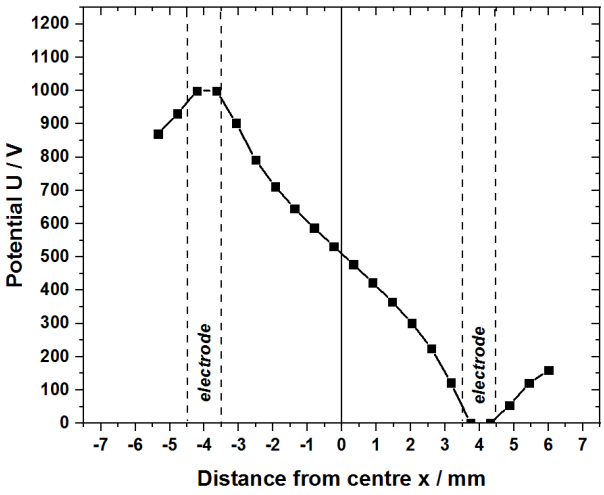

Figure 3-2
Distribution of Electric field strength E and scalar electric potential *U*, with an applied voltage of 1000 V over two electrodes of 0.7 mm diam., and 8 mm electrode spacing.

3.1.2 Electric field-strength distribution E

Figure 3-3 shows the distribution of Electric field-strength **E,** modelled between two needle electrodes with a diameter of 1 mm inserted into muscle tissue with conductivity 0.20 S/m. The electrodes of steel with a conductivity of $6.2 \cdot 10^6$ S/m were separated 8 mm with an applied voltage of 1000 V at the left electrode and 0V at the right.

Figure 3-4 displays the profile of electric field-strength distribution along a horizontal line through the electrodes. The average electric field in the region of ± 2 mm from the centre estimated by modelling with various tissue conductivities shown in Figure 3-5 is about 1050 V/cm independent of conductivity.

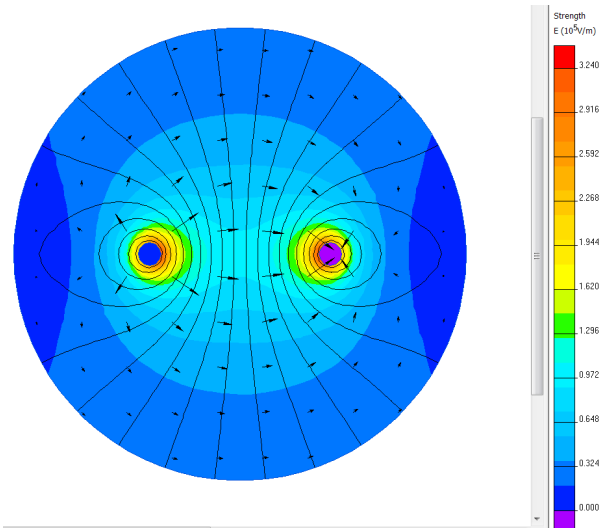

Figure 3-3
Distribution of Electric field strength E with an applied voltage of 1000 V over two electrodes of 1mm diam. and 8 mm electrode spacing in muscle tissue with conductivity 0.20 S/m.

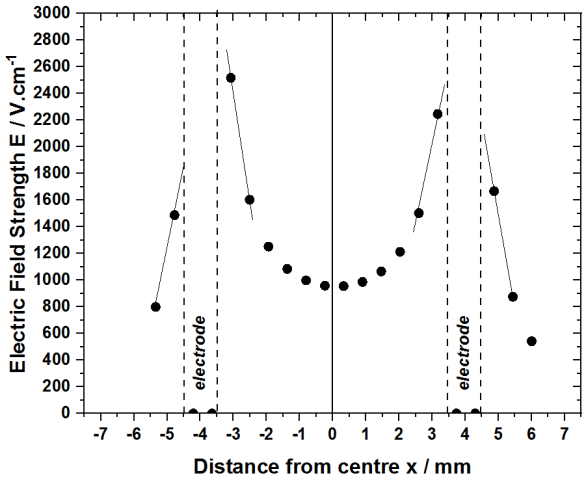

Figure 3-4
Distribution of Electric field strength E with an applied voltage of 1000 V over two electrodes of 1.0 mm diam., and 8 mm electrode spacing in muscle tissue with conductivity 0.20 S/m. The average field strength in the region ± 2 mm between the electrodes is about 1150 ± 90 V/cm.

Figure 3-5 shows the average electric field strength in tissue of various conductivities in the region of ± 2 mm between two electrodes of 1 mm diameter, and 8 mm electrode spacing with an applied voltage between the electrodes of1000 V. The average electric field strength between the electrodes is slightly above 1000 V/cm independently of the tissue conductivity.

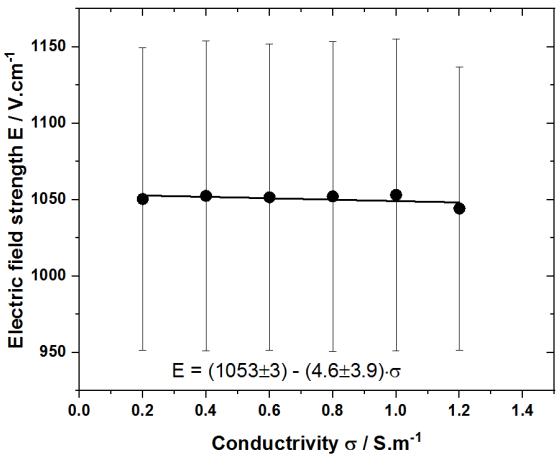

Figure 3-5

The average Field strength in tissue of various conductivity in the central region of ± 2 mm between two electrodes of 1 mm diam., and 8 mm electrode spacing with an applied voltage between the electrodes of 1000 V.

3.1.3 Current density distribution j

Figure 3-6 shows the distribution of electric current density **j** modelled between two needle electrodes with a diameter of 1 mm inserted in muscle tissue with conductivity 0.20 S/m. The electrodes of steel with a conductivity of $6.2 \cdot 10^6$ S/m were separated 8 mm with an applied voltage of 1000 V at the left electrode and 0V at the right.

The average electric current density in the region of ± 2 mm from the centre estimated by modelling with various tissue conductivities σ, increase linearly with conductivity. The current density expressed in A.cm^{-2} corresponds approximately to the recorded current between the electrodes.

$$I \approx 10 \cdot \sigma$$

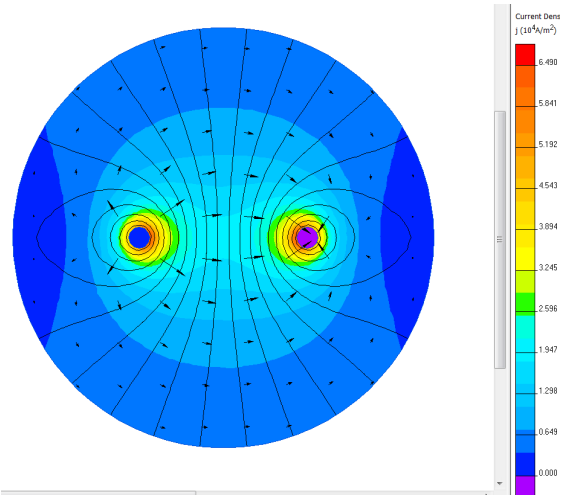

Figure 3-6
Distribution of current density **j** with an applied voltage of 1000 V over two electrodes of 1 mm diam. and 8 mm electrode spacing in muscle tissue with conductivity 0.20 S/m.
The average current distribution in the region ± 2 mm between the electrodes is about 2 A.cm^{-2}.

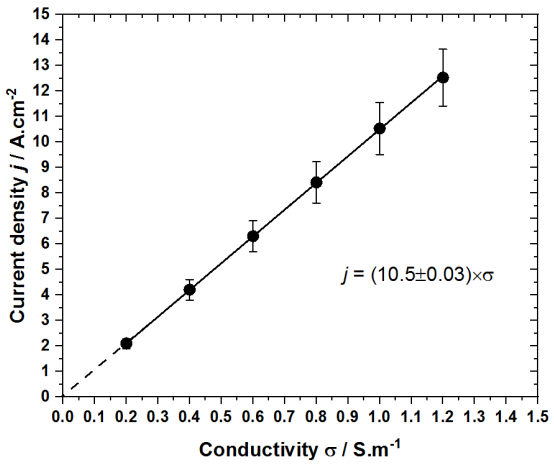

Figure 3-7 The average current density j in tissue of various conductivities in the region of ± 2mm between two electrodes of 1 mm diameter, and 8 mm electrode spacing at an applied voltage between the electrodes of 1000 V.

3.1.4 Distribution of absorbed power density P

Figure 3-8 shows the absorbed power density P_v (W/m^3) between two needle electrodes with a diameter of 1 mm inserted into muscle tissue with conductivity 0.20 S/m. The electrodes of steel with a conductivity of 6.2·10^6 S/m were separated 8 mm with an applied voltage of 1000 V at the left electrode and 0 V at the right.

The average absorbed power density along a horizontal line in the region ± 2 mm between the electrodes is about 2.22·10^9 W.m^{-3}, which corresponds to 2.22·10^6 W/kg.

For a 100 µs long pulse of 1000 V/cm amplitude the absorbed energy density is 2.22·10^2 J/kg = 0.22 J/g = 0.22 Mir$^{*)}$.

$^{*)}$ The unit for absorbed dose in radiation therapy is named "*gray*", (1 Gy = 1 J/kg) to honour Louis Harold Gray. The unit for absorbed dose in electro chemo therapy is suggested to be named "*mir*", (1 Mir = 1 J/g), to honour Lluis M Mir for his great contributions to the field of electrochemotherapy.

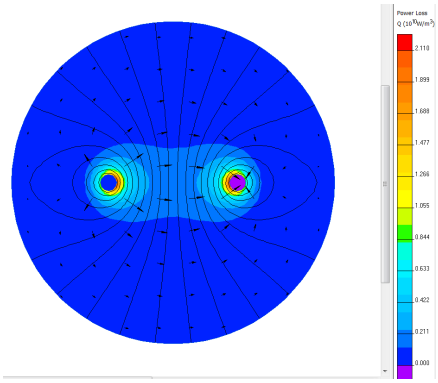

Figure 3-8

Distribution of absorbed power density P_v W/m^3 with an applied voltage of 1000 V over two electrodes of 1mm diam. and 8 mm electrode spacing in muscle tissue with conductivity 0.20 S/m.

Specific absorbed energy and temperature increase

The specific absorbed energy SAE is calculated from the following expression

$$SAE = \frac{\sigma \cdot E^2}{\rho} \cdot t_p \cdot N \quad [J.kg^{-1}]$$

where

σ is the tissue conductivity for the tissue [S/m]
E is the electric field strength [V/m]
t_p is the pulse length [s]
N is the number of applied pulses
ρ is the density of tissue (muscle 1060) kg.m^{-3}

The following equation predicts the conductivity of the tissue after electroporation

$$\sigma_{after} = \sigma_{before} \cdot R_{before}/R_{after}$$

The average specific absorbed energy in tissue of various conductivity of a single 100 µs long pulse of 1000 V amplitude varies with the conductivity in the region of ± 2 mm between two electrodes of 1 mm diam., and 8 mm electrode spacing of the medium as:

Equation SAE = (1.11 ± 0.006)×σ; J/g
R-Square (COD) = 0.9998

The value for the heat capacity of muscle issues is 3421 ± 460 [J.kg^{-1}.°C^{-1}] {Hasgall, 2015 #5293}. The temperature rise in the tissue after in tissue of various conductivity of a single 100 µs long pulse of 1000 V amplitude varies with the conductivity in the region of ± 2 mm between two electrodes of 1 mm diam., and 8 mm electrode spacing of the medium is:

Equation ΔT = (0.33±0.05)×σ; °C

Thus the electro pulse therapy procedure does not do not induce any significant hyper-thermic effects.

3.2 Distribution of U, E, j and P_V at the second pulse

As seen in Figure 3-4, the electric field strength E is quite high around the electrodes, in a region within 0.5 - 2 mm radius. After the first pulse the conductivity in this volume close to the electrodes will increase due to the high field strength. In order to take this effect into account, the conductivity after the first pulse is given a value of 1 S/m for a region within an outer radius of 1.5 mm around the electrode. The figure 3-9 shows a model with a region of 3 mm diameter around the electrode with the conductivity of 1 S/m, while the rest of tissue has a conductivity of 0.2 S/m.

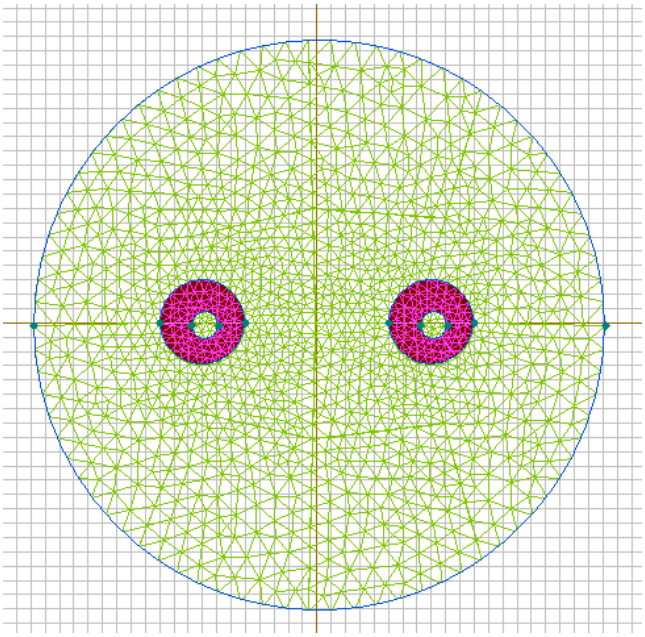

Figure 3-9

The model in a grid of 0.5 mm, with an area of 0.5 -1.5 mm radius around the electrode with the conductivity of 1 S/m, while the rest of tissue has a conductivity of 0.2 S/m..

3.2.1 Potential distribution U

Figure 3-10 below shows the distribution of the potential U of the 2nd pulse with an applied voltage of 1000 V over two electrodes of 1 mm diameter and 8 mm electrode spacing. The conductivity is set to 1 S/m in a region of 3 mm outer diameter around the electrode while the rest of tissue has a conductivity of 0.2 S/m.

Figure 3-11 displays the centre x-distribution of scalar electric potential *U*, with an applied voltage of 1000 V over two electrodes of 1 mm diameter and 8 mm electrode spacing. The conductivity is set to 1 S/m in a region of 3 mm outer diameter around the electrode while the rest of tissue has a conductivity of 0.2 S/m.

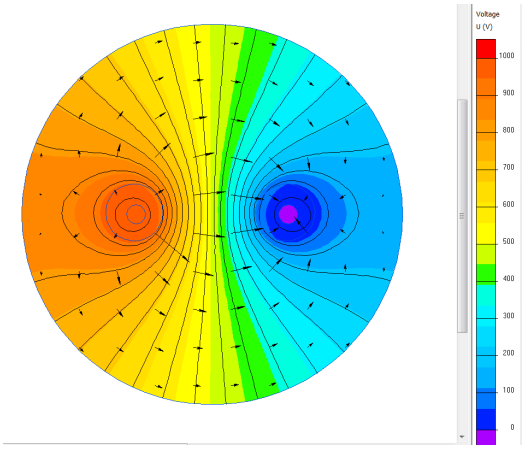

Figure 3-10
The electric potential U distribution at the 2nd pulse with an applied voltage of 1000 V over two electrodes of 1 mm diameter and 8 mm electrode spacing. The conductivity is set to 1 S/m in a region of 3 mm outer diameter around the electrode while the rest of tissue has a conductivity of 0.2 S/m.

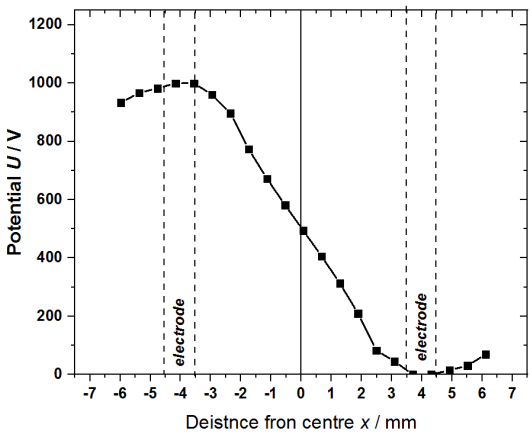

Figure 3-11
Centre x-distribution of scalar electric potential *U*, with an applied voltage of 1000 V over two electrodes of 1 mm diameter and 8 mm electrode spacing. The conductivity is set to 1 S/m in a region of 3 mm outer diameter around the electrode while the rest of tissue has a conductivity of 0.2 S/m.

3.2.2 Electric Field E distribution

Figure 3-12 shows the distribution of electric field strength E at the 2nd pulse with an applied voltage of 1000 V over two electrodes of 1 mm diameter and 8 mm electrode spacing. The conductivity is set to 1 S/m in a region of 3 mm outer diameter around the electrode while the rest of tissue has a conductivity of 0.2 S/m.

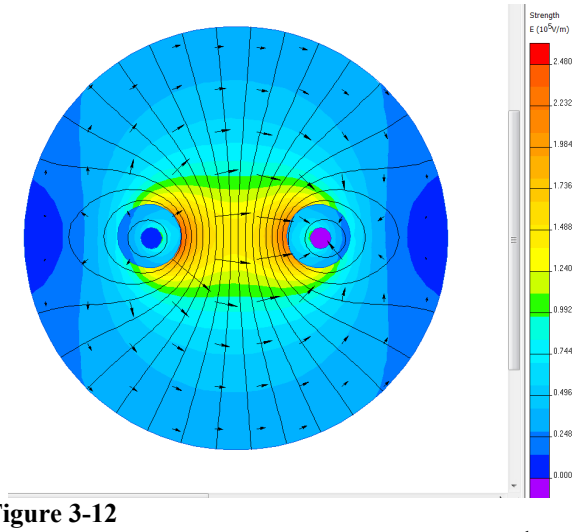

Figure 3-12
Distribution of electric field strength E at the 2nd pulse with an applied voltage of 1000 V over two electrodes of 1 mm diameter and 8 mm electrode spacing. The conductivity is set to 1 S/m in a region of 3 mm outer diameter around the electrode while the rest of tissue has a conductivity of 0.2 S/m.

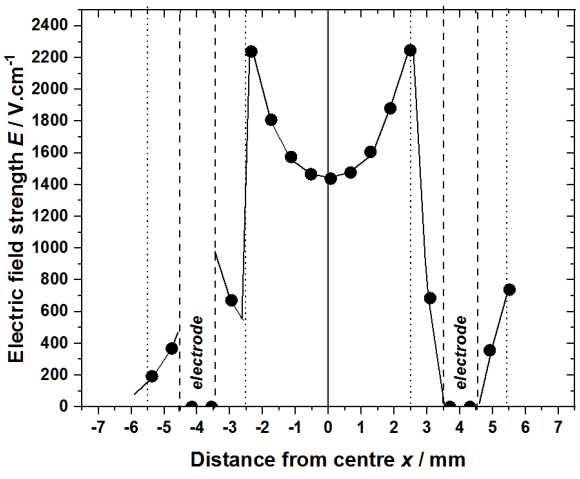

Figure 3-13
Profile of the electric field strength ***E*** along the centre ***x***-axis, with an applied voltage of 1000 V over two electrodes of 1 mm diam., and 8 mm electrode spacing. The conductivity in region of 3 mm diameter around the electrode is increased to 1 S/m due to the effect of the first pulse, while the rest of tissue has a conductivity of 0.2 S/m.

Figure 3-13 displays the profile of the electric field strength ***E*** along the centre ***x***-axis, with an applied voltage of 1000 V over two electrodes of 1 mm diam., and 8 mm electrode spacing. The conductivity in region of 3 mm diameter around the electrode is increased to 1 S/m due to the effect of the first pulse, while the rest of tissue has a conductivity of 0.2 S/m.

The average field strength along a horizontal line in the region ± 2 mm between the electrodes is about 1750 V/cm, compared to 1150 V/cm in the first pulse.

3.2.3 Electric current density j distribution

Figure 3-17 shows the distribution of electric current distribution ***j*** at the 2nd pulse with an applied voltage of 1000 V over two electrodes of 1 mm diameter and 8 mm electrode spacing. The conductivity is set to 1 S/m in a region of 3 mm outer diameter around the electrode while the rest of tissue has a conductivity of 0.2 S/m.

Figure 3-18 display the average current density profile ***E*** along the centre ***x***-axis in the region ± 2 mm between the electrodes. The average is about 3.5 A.cm^{-2}, compared to 2 A.cm^{-2} in the first pulse. Thus in order to keep the current density at the level of the first pulse the applied voltage amplitude of the second pulse should be reduced.

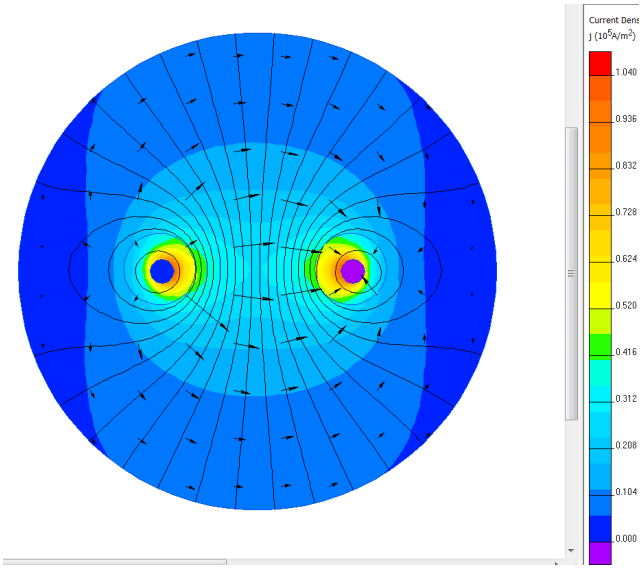

Figure 3-14
Distribution of electric current distribution ***j*** at the 2nd pulse with an applied voltage of 1000 V over two electrodes of 1 mm diameter and 8 mm electrode spacing. The conductivity is set to 1 S/m in a region of 3 mm outer diameter around the electrode while the rest of tissue has a conductivity of 0.2 S/m.
The average current density in the region ± 2 mm between the electrodes is about 3.5 A.cm^{-2}

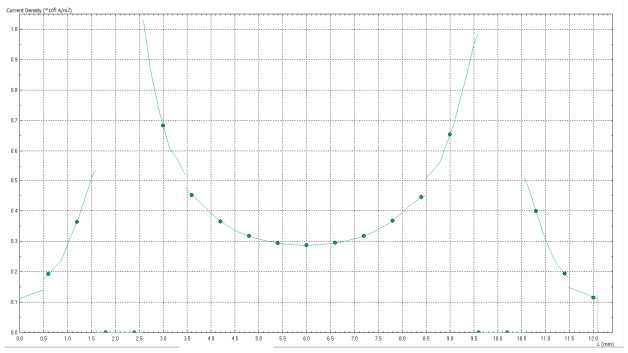

Figure 3-15
QF plot of Centre x-distribution of electric current distribution ***j*** at the 2nd pulse with an applied voltage of 1000 V over two electrodes of 1 mm diameter and 8 mm electrode spacing. The conductivity is set to 1 S/m in a region of 3 mm outer diameter around the electrode while the rest of tissue has a conductivity of 0.2 S/m.

3.2.4 Absorbed power density P_V distribution

Figure 3-16 shows the distribution of **absorbed power density P_V** distribution at the 2nd pulse with an applied voltage of 1000 V over two electrodes of 1 mm diameter and 8 mm electrode spacing. The conductivity is set to 1 S/m in a region of 3 mm outer diameter around the electrode while the rest of tissue has a conductivity of 0.2 S/m.

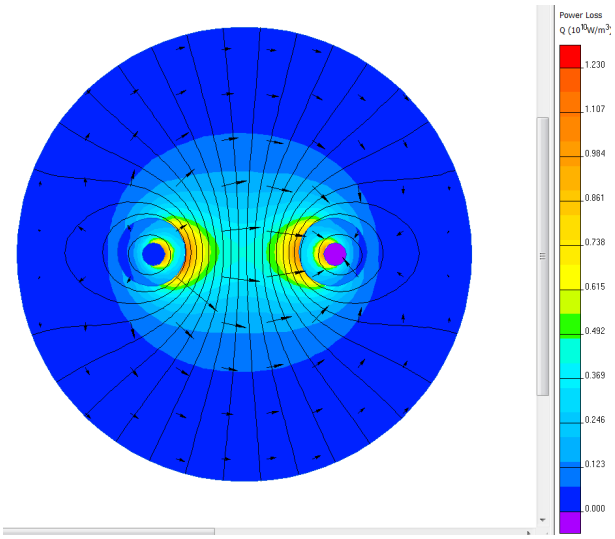

Figure 3-16
Distribution of **absorbed power density P_V** distribution at the 2nd pulse with an applied voltage of 1000 V over two electrodes of 1 mm diam. and 8 mm electrode spacing and a region of 3 mm diameter around the electrode with the conductivity of 1 S/m while the rest of tissue has a conductivity of 0.2 S/m.

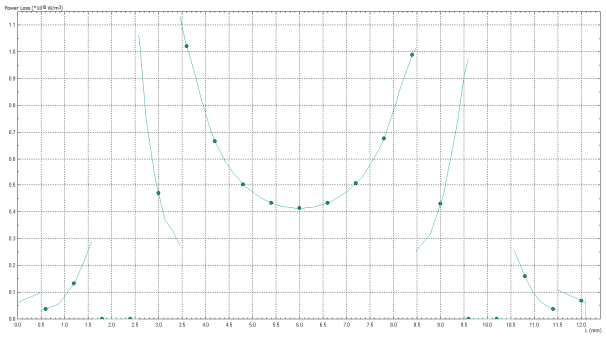

Figure 3-17
QF plot of Centre x-distribution of **absorbed power density P_V** at the 2nd pulse with an applied voltage of 1000 V over two electrodes of 1 mm diam. and 8 mm electrode spacing and a region of 3 mm diameter around the electrode with the conductivity of 1 S/m while the rest of tissue has a conductivity of 0.2 S/m

Figure 3-17 show the QF-plot of the Centre x-profile of **absorbed power density P_V** at the 2nd pulse with an applied voltage of 1000 V over two electrodes of 1 mm diameter and 8 mm electrode spacing. The conductivity is set to 1 S/m in a region of 3 mm outer diameter around the electrode while the rest of tissue has a conductivity of 0.2 S/m.

The average **absorbed power density** in the region ± 2 mm between the electrodes is about 0.63 J/g compared to 0.22 J/g in the first pulse.

4. Discussions

Figure 4-1 shows the pulse train used in the European Standard Operational Protocol (ESOPE) for electrochemotherapy. The ESOPE claims a pulse sequence of 8 pulses, each with an amplitude of 1000 V/cm applied over the distance between the electrodes, and a pulse-length of 0.1 ms, delivered at a frequency of 5 kHz (Marty et al., 2006). According to the result of the present QF simulation, the average pulse strength after the initial pulse increases above the recommended 1000 V/cm, in the centre between the electrodes which might cause non-reversible electroporation in the whole target volume.

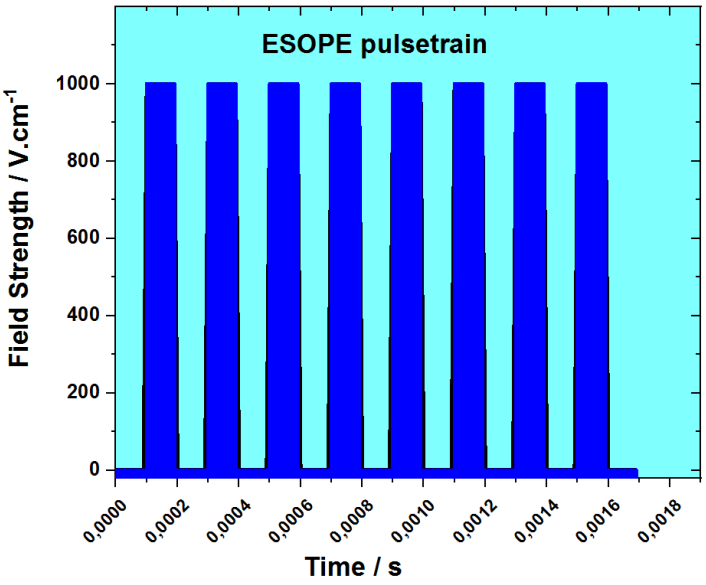

Figure 4-1
The ESOPE pulse train

The extensively increase of the electric-field in the centre of the target volume could be avoided by decreasing the amplitude of the second and following pulses in the pulse train. Figure 3-19 shows an example of a pulse sequence with exponentially decreasing pulse amplitude with a time constant of 1 ms. A pulse sequence with exponentially decreasing pulse amplitude an excellent therapy efficiency of adenocarcinoma implanted in rat liver with a high degree of immune response, resulting in anti-metastatic effect (Engstrom et al., 2001).

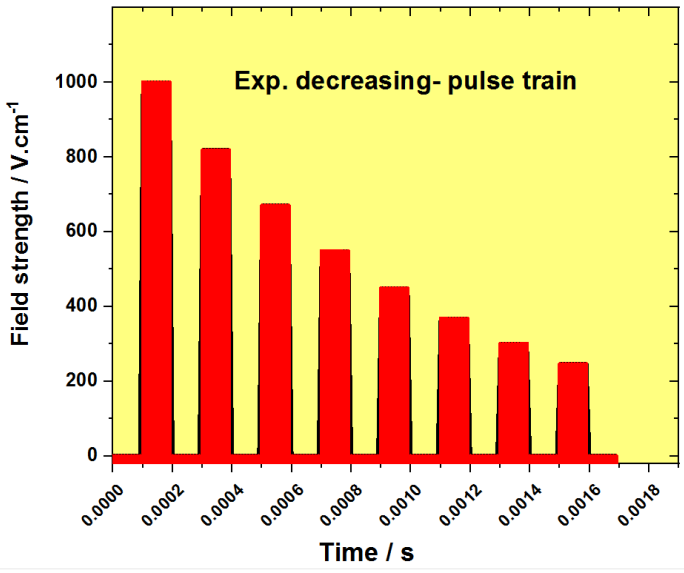

Figure 4-2
Pulse train of Exponentially decreasing E-field that could preferentially apply to Electro-pulse therapy.

The concept of using a pulse-train of decreasing pulse amplitude has been further explored by collaboration with Mohan Frick in the development of Dynamic-Electro Enhanced Chemotherapy, D-EECT™. A special device IQWave™ (Scandinavian, Chemotech AB Lund Sweden) applying the D-

EECT™ protocol has been used together with an electrode device with four needle electrodes, in a clinical case study performed in India (Frick et al., 2019 , Kalavathy et al., 2018, Frick and Persson, 2020). The study involved 23 patients treated in a total of 38 sessions of D-EECT™ at four different cancer centres. The treatment response to a total of 66 tumours of various sizes and different histological types was as follows: complete remission's CR=18%, partial remissions PR=82%, that corresponds to objective responses of 100%. No progressive disease was recorded.

In a recent electro chemo therapy study of 43 patients with recurrent mucosal head and neck tumours, treated according to the ESOPE protocol, the SCC patients split into one group with a nodule diameter less than 3 cm, and another group with nodules larger than 3 cm (Plaschke et al., 2017). The objective responses in the various groups of patients were 71% for tumours < 3cm, and 60% for tumours >3cm. However progressive disease was recorded in 7% of the cases with tumours <3cm, and 10 % with tumours >3cm. In the Kalavathy work, the sizes of the SCC nodules were in the range of 5-6 cm with no reported cases of progressive disease (Kalavathy et al., 2018).

Another recent report on an electro chemotherapy treatment according to the ESOPE protocol at 10 European cancer centres involves 90 patients with cutaneous recurrence from breast tumours. The objective response to electro chemotherapy was 86% for breast tumours nodules of < 3cm in size, and 62% for tumours > 3cm. Progressive disease was found in 1 % of the group of patients with tumours smaller than 3cm, and in 6 % with tumours >3cm (Matthiessen et al., 2018). In the Kalavathy study of breast cancer patients with nodules in the range of 7-8 cm, the objective response was 100 % with no cases of progressive disease (Kalavathy et al., 2018).

The differences in the clinical responses between the ESOP and D-EEPC protocol might be explained by the overexposure of electric fields in the ESOPE protocol. This may cause elevated non reversible electroporation resulting in immune suppression, reflected on the higher proportion of progressive disease in the ESOPE studies although the tumours are smaller than in the D-EEPC study.

Acknowledgement
The authors wish to thank the QuickField support team for the temporary license of the program, Version 6.3.2 (Tera Analysis Ltd. http://quickfield.com), without which this work could not have been performed.

References

CHAZAL, M., BENCHIMOL, D., BAQUE, P., PIERREFITE, V., MILANO, G., & & BOURGEON, A. 1998. Treatment of hepatic metastases of colorectal cancer by electrochemotherapy: an experimental study in the rat 124,**,** 536-540.

ENGSTROM, P. E., IVARSSON, K., TRANBERG, K. G., STENRAM, U., SALFORD, L. G. & PERSSON, B. R. R. 2001. Electrically mediated drug delivery for treatment of an adenocarcinoma transplanted into rat liver. *Anticancer Research,* 21**,** 1817-1822.

FRICK, M. & PERSSON, B. R. R. 2020. *A pulse generating device for delivery of electrical pulses to a desired tissue of a mammal (Patent)*. Sweden,SE 542 514 C2.

FRICK, M., PERSSON, B. R. R. & MARNFELDT, J. 2019. *An electrode device and a needle electrode for use in delivery of electrical pulses to a desired tissue of a mammal (Patent)*. Sweden,SE 541 651 C2.

HELLER, R., JAROSZESKI, M., GLASS, F., PULEO, C., DECONTI, R., REINTGEN, D. & GILBERT, R. 1997. Enhanced delivery of bleomycin using electric fields for the effective treatment of skin malignancies. *Proceedings of the American Association for Cancer Research Annual Meeting,* 38**,** 259-259.

HELLER, R., JAROSZESKI, M. J., REINTGEN, D. S., PULEO, C. A., DECONTI, R. C., GILBERT, R. A. & GLASS, L. F. 1998. Treatment of cutaneous and subcutaneous tumors with electrochemotherapy using intralesional bleomycin. *Cancer,* 83**,** 148-157.

HYACINTHE, M., JAROSZESKI, M. J., DANG, V. V., COPPOLA, D., KARL, R. C., GILBERT, R. A. & HELLER, R. 1999. Electrically enhanced drug delivery for the treatment of soft tissue sarcoma. *Cancer,* 85**,** 409-417.

JAROSZESKI, M., GILBERT, R., DANG, V., HICKEY, J. & HELLER, R. 1997a. In vivo electroporation for drug delivery to rat hepatomas. *Proceedings of the American Association for Cancer Research Annual Meeting,* 38**,** 259-260.

JAROSZESKI, M. J., GILBERT, R. A. & HELLER, R. 1997b. In vivo antitumor effects of electrochemotherapy in a hepatoma model. *Biochimica Et Biophysica Acta-General Subjects,* 1334**,** 15-18.

JAROSZESKI, M. J., ILLINGWORTH, P., POTTINGER, C., HYACINTHE, M. & HELLER, R. 1999. Electrically mediated drug delivery for treating subcutaneous and orthotopic pancreatic adenocarcinoma in a hamster model. *Anticancer Research,* 19**,** 989-994.

KALAVATHY, G., GURUMURTHY. G., RAJESH, K., SARAVANAN, ASOKE , M. & PERSSON, B. R. R. 2018. Dynamic-ElectroEnhanced Chemotherapy brings relief to palliative patients with large tumour burden. *Trends in Cancer Research,* 13**,** 29-41.

MARTY, M., SERSA, G., GARBAY, J. R., GEHL, J., COLLINS, C. G., SNOJ, M., BILLARD, V., GEERTSEN, P. F., LARKIN, J. O., MIKLAVCIC, D., PAVLOVIC, I., PAULIN-KOSIR, S. M., CEMAZAR, M., MORSLI, N., RUDOLF, Z., ROBERT, C., O'SULLIVAN, G. C. & MIR, L. M. 2006. Electrochemotherapy - An easy, highly effective and safe treatment of cutaneous and subcutaneous metastases: Results of ESOPE (European Standard Operating Procedures of Electrochemotherapy) study. *Ejc Supplements,* 4**,** 3-13.

MATTHIESSEN, L. W., KESHTGAR, M., CURATOLO, P., KUNTE, C., GRISCHKE, E. M., ODILI, J., MUIR, T., MOWATT, D., CLOVER, J. P., LIEW, S. H., DAHLSTROEM, K., NEWBY, J., LETULE, V., STAUSS, E., HUMPHREYS, A., BANERJEE, S., KLEIN, A., ROTUNNO, R., DE TERLIZZI, F. & GEHL, J. 2018. Electrochemotherapy for Breast Cancer-Results From the INSPECT Database. *Clinical Breast Cancer,* 18**,** E909-E917.

MIR, L. M., GLASS, L. F., SERSA, G., TEISSIE, J., DOMENGE, C., MIKLAVCIC, D., JAROSZESKI, M. J., ORLOWSKI, S., REINTGEN, D. S., RUDOLF, Z., BELEHRADEK, M., GILBERT, R., ROLS, M. P., BELEHRADEK, J., BACHAUD, J. M., DECONTI, R., STABUC, B., CEMAZAR, M., CONINX, P. & HELLER, R. 1998. Effective treatment of cutaneous and subcutaneous malignant tumours by electrochemotherapy. *British Journal of Cancer,* 77**,** 2336-2342.

OKINO, M. & MOHRI, H. 1987. Effects of a high-voltage electrical impulse and an anticancer drug on in vivo growing tumors. *Jpn.J.Cancer Res.,,* 78,**,** 1319-1321.

OKINO, M., TOMIE, H., KANESADA, H., MARUMOTO, M., ESATO, K. & SUZUKI, H. 1992. Optimal electric conditions in electrical impulse chemotherapy. *Japanese Journal of Cancer Research,* 83**,** 1095-1101.

PLASCHKE, C. C., BERTINO, G., MCCAUL, J. A., GRAU, J. J., DE BREE, R., SERSA, G., OCCHINI, A., GROSELJ, A., LANGDON, C., HEUVELING, D. A., CEMAZAR, M., STROJAN, P., LEEMANS, C. R., BENAZZO, M., DE TERLIZZI, F., WESSEL, I. & GEHL, J. 2017. European Research on Electrochemotherapy in Head and Neck Cancer (EURECA) project: Results from the treatment of mucosal cancers. *European Journal of Cancer,* 87**,** 172-181.

RAMIREZ, L. H., ORLOWSKI, S., AN, D., BINDOULA, G., DZODIC, R., ARDOUIN, P., BOGNEL, C., BELEHRADEK, J., MUNCK, J. N. & MIR, L. M. 1998. Electrochemotherapy on liver tumours in rabbits. *British Journal of Cancer,* 77**,** 2104-2111.

SALFORD, L. G., PERSSON, B. R. R., BRUN, A., CEBERG, C. P., KONGSTAD, P. C. & MIR, L. M. 1993. A new Brain Tumour Therapy Combining Bleomycin with in vivo Electropermeabilization. *Biochemical and Biophysical Research Communications,* 194**,** 938-943.